Laser and Particle Beams (2009), *27*, 485–490. Printed in the USA.

doi:10.1017/S0263034609990218

Quasi-monoenergetic proton beam generation from a double-layer solid target using an intense circularly polarized laser

J.H. BIN,[1] A.L. LEI,[1] X.Q. YANG,[1] L.G. HUANG,[1] M.Y. YU,[2] WEI YU,[1] AND K.A. TANAKA[3]

[1]Shanghai Institute of Optics and Fine Mechanics, Chinese Academy of Sciences, Shanghai, China
[2]Institute for Fusion Theory and Simulation, Zhejiang University, Hangzhou, China
[3]Graduate School of Engineering, Osaka University, Osaka, Japan

(Received 6 March 2009; Accepted 12 June 2009)

Abstract

Monoenegetic ion beam generation from circularly polarized laser-pulse interaction with a double-layer target is considered. The front layer consists of heavy-ion plasma, and the rear layer is a small thin coating of light-ion plasma. Particle-in-cell simulation shows that the multi-dimensional effects in the ion radiation pressure acceleration are avoided and a highly monoenergetic light-ion beam can be produced. Our simulations reveal that the charge-mass ratio of heavy ions in the front layer and the thicknesses of both layers can strongly affect the proton energy spectra.

Keywords: Circularly polarized laser; Double-layer solid target; PIC simulation; Quasi-monoenergetic proton generation

1. INTRODUCTION

With the rapid advances in laser technology, energetic-ion-beam production from intense-laser interaction with matter have attracted much attention because of its compactness and many potential applications, such as in ion cancer therapy (Malka *et al.*, 2004; Linz & Alonso, 2007; Yogo *et al.*, 2009), fast ignition in inertial confinement fusion (ICF) (Roth *et al.*, 2001), fast-beam injection in conventional accelerators (Krushelnik *et al.*, 2000), proton radiography and imaging (Borghesi *et al.*, 2002; Cobble *et al.*, 2002; Breschi *et al.*, 2004), etc. Most of these applications require ion beams with small energy spread $\Delta\varepsilon/\varepsilon$. For example, for cancer therapy, a proton beam with $\Delta\varepsilon/\varepsilon \leq 2\%$ would be needed (Khoroshkov & Minakova, 1998; Kraft, 2001). However, energetic ion beams obtained in the experiments usually have large (say 100%) $\Delta\varepsilon/\varepsilon$.

With specially structured targets, quasi-monoenergetic ion beams with $\Delta\varepsilon/\varepsilon \leq 20\%$ have been achieved using linearly polarized (LP) laser pulses (Hegelich *et al.*, 2006; Schwoerer *et al.*, 2006). Both works were based on the ion acceleration mechanism target normal sheath acceleration (TNSA) (Wilks *et al.*, 2001; Esirkepov *et al.*, 2002; Flippo *et al.*, 2007; Nickles *et al.*, 2007). In TNSA, the hot electrons are generated by the LP laser pulse at the target front and are transported through the target to the backside vacuum, forming a strong electrostatic space-charge sheath field there. The sheath field is normal to the target rear surface and can accelerate some of the ions in the latter to high energy. Recently, with LP laser pulses, Yin *et al.* (2006, 2007) have shown in the particle-in-cell (PIC) simulations that monoenergetic ion beams up to GeV are generated due to laser breakout afterburner (BOA) acceleration mechanism (Davis & Petrov, 2009).

Using circularly polarized (CP) laser pulses, a new mechanism radiation pressure acceleration (RPA) was considered for monoenergetic ion beam generation (Macchi *et al.*, 2005; Kado *et al.*, 2006; Liseikina & Macchi, 2007; Zhang *et al.*, 2007; Klimo *et al.*, 2008; Robinson *et al.*, 2008; Yan *et al.*, 2008). Without high-frequency oscillating component of the $v \times B$ force for a CP laser pulse, there is no heating originating from the hot electron oscillations when it is normally incident on a target (Macchi *et al.*, 2005). The electrons are pushed forward steadily and compressed by the light pressure. An intense electrostatic field is thus formed, which then accelerates ions inside the target. One-dimensional (1D) simulations show that fairly monoenergetic ion beams can be generated (Macchi *et al.*, 2005; Zhang *et al.*, 2007; Klimo *et al.*, 2008; Robinson *et al.*, 2008). However, in reality higher-dimensional effects

Address correspondence and reprint requests to: Anle Lei, Shanghai Institute of Optics and Fine Mechanics, Chinese Academy of Sciences, Shanghai 201800, China. E-mail: lal@siom.ac.cn

such as hole boring and filamentation (Liseikina & Macchi, 2007; Klimo *et al.*, 2008; Robinson *et al.*, 2008; Yan *et al.*, 2008) can significantly increase $\Delta\varepsilon/\varepsilon$ and thus reduce the quality of the ion beam.

In this paper, we show by two-dimensional (2D) PIC simulation that a CP laser pulse of intensity 2.5×10^{21} Wcm^{-2} irradiating a double-layer (DL) target can produce a highly localized monoenergetic ion beam of $\sim$156 MeV with $\Delta\varepsilon/\varepsilon \approx 4\%$. The target is made up of two layers of different materials. The intense CP laser is normally incident on the dense front layer of heavy ions. The rear layer is a thin dot of light ions. The front-layer electrons driven forward in the overdense plasma by the laser ponderomotive force form in front of the pulse a thin highly compressed electron layer. An electron depletion region (EDR) with very intense space-charge field is thus created (Macchi *et al.*, 2005). When it propagates to the rear surface of the front layer of heavy ions, light ions in the rear layer are then accelerated. With the DL target, the multidimensional effects in the light ion RPA are avoided and a highly monoenergetic light-ion beam can be produced. The regime of ion acceleration here is also quite different from that of the existing TNSA scheme (Schwoerer *et al.*, 2006).

2. BRIEF ARGUMENT

As mentioned above, when a CP laser pulse is normally incident on the front layer, the electrons there are ponderomotively driven forward and compressed into a thin electron layer, whose spatial extent is on the order of the skin depth $l_s = c/\omega_p$, where c is the light speed and ω_p is the plasma frequency. While the intense space-charge electrostatic field is formed in front of the laser increases with time, further numbers of electrons are kicked into the compression layer until it reaches a maximum when the electrostatic pressure balances the light pressure. The optimum thickness of the front target layer can be obtained when the highest space-charge field is formed just at its rear surface, and can be written as (Yin *et al.*, 2008) $d_{\rm opt} = \sqrt{I_L/\pi c}/en_{e1}$, where I_L is the laser pulse intensity and n_{e1} is the initial electron density for the front layer. This intense space-charge field then accelerates the light ions in the rear layer. Since the laser pulse and its ponderomotive force are spatially nonuniform, which may lead to nonuniformity in the space-charge field, the thickness d_2 of the rear layer is taken to be close to the skin depth l_s and its transverse size is taken to be smaller than the laser-pulse waist. We define that in the present scheme, the acceleration phase is separated from the space-charge-field-establishing phase, so that undesirable longer-timescale effects such as hole-boring, filamentation, etc. are avoided and a light-ion beam of high energy and small energy spread can be obtained.

3. SIMULATION PARAMETERS

To verify the above argument, we have carried out simulations using the 2D PIC code LAPINE (Xu *et al.*, 2002). A Gaussian CP laser pulse with wavelength $\lambda_0 = 1$ μm and beam waist radius $\omega_0 = 4\lambda_0$ is normally incident from the left side. The laser amplitude $a = eA/m_e c^2$, where A is the vector potential, e and m_e are the electron charge and mass, respectively, and c is the light speed, rises from zero to 30 (corresponding to a laser intensity of $I_L = 2.5 \times 10^{21}$ Wcm^{21}) in one laser period T_0 and remains constant for $30T_0$. The simulation box is $60\lambda_0$ in the laser propagation (x) direction and $20\lambda_0$ in the y direction. The front layer consists of a carbon plasma with an electron density $n_{e1} = 10n_c$, where n_c is the critical density, and the rear-layer consists of protons with an electron density $n_{e2} = n_c$. The front layer is at $x = 20\lambda_0$ and has a diameter $D_1 = 10\lambda_0$ and thickness $d_1 = 1\lambda_0$ (which is near the optimum thickness $d_{\rm opt}$). The rear, or proton, layer has a diameter $D_2 = 1\lambda_0$ and thickness $d_2 = 0.05\lambda_0$ (which is near the skin depth $l_s = c/\omega_p$) is attached directly to the rear side of the front layer. That is, the parameters chosen are near that for optimum ion beam production as estimated above.

4. SIMULATION RESULTS AND DISCUSSION

Figure 1a shows the evolution of the energy spectra of protons produced by the DL target. One can see that a highly monoenergetic proton beam of $\sim$156 MeV and $\Delta\varepsilon/\varepsilon \leq 4\%$ is produced by the laser plasma interaction, and it maintains its monoenergetic characteristics as it is accelerated, even up to $t = 90T_0$. For comparison, Figure 1b shows the evolution of the energy spectrum of the protons produced from a single-layer proton target of thickness of $1\lambda_0$ and density of $10n_c$. We see that in this case, the proton energy peaks at an early stage ($t < 30T_0$) with a broad spectrum, and the peak disappears quickly as the proton beam propagates forward.

The ratio Z_1/A_1 of the charge number to the atomic mass of the heavy ions in the front-layer obviously plays a crucial role in accelerating the much lighter protons in the rear layer. The evolution of the electrostatic space-charge field established by the laser-expelled front-layer electrons is shown in Figure 2a. We see that the field profile is almost linear in both its rising and falling segments. For convenience, one can divide the field into two regions (Macchi *et al.*, 2005): I and II, as shown in Figure 2b. In region I with the rising field, the protons have lower velocities and never pass through the peak of field. On the other hand, in region II with the falling field, the protons are accelerated and are compressed. In the DL, the space-charge field established by the laser displaced front-layer electrons can accelerate the heavy ions there to a velocity (Macchi *et al.*, 2005) $2v_0$ where $v_0/c = \sqrt{Z_1 m_e n_c/A_1 m_p n_{e1} a}$, and m_p is the proton mass. In the time $t = (d_1 + d_2)/2v_0$ for the heavy ions to pass through the DL, the protons will obtain a velocity $v_1 = (Z_2 eE_0/2A_2 m_p)((d_1 + l_s)/2v_0)$, where $E_0 = 4\pi en_{e1}d_1$ is the peak value of the electrostatic field and we have substituted d_2 by l_s. Therefore, there can exist three different cases.

https://doi.org/10.1017/S0263034609990218 Published online by Cambridge University Press

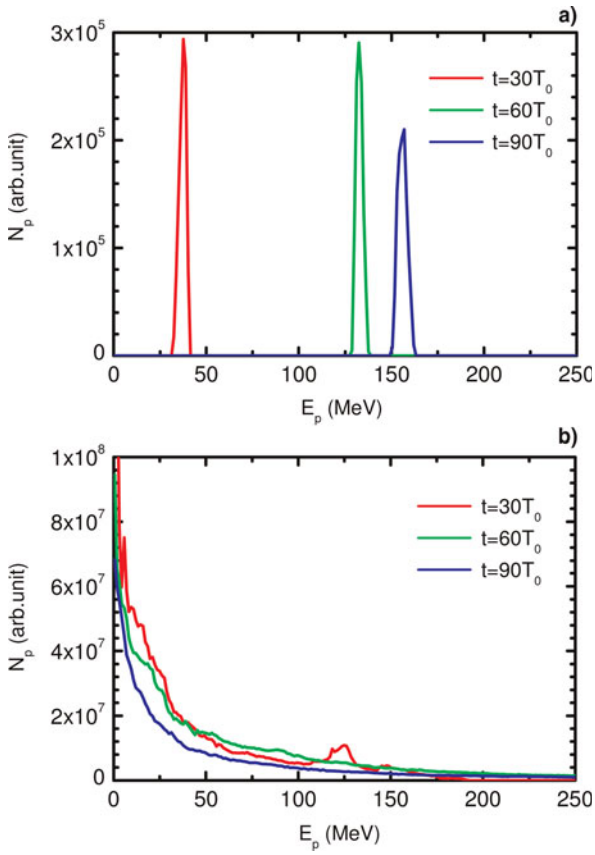

Fig. 1. (Color online) The proton energy spectra from 2D PIC simulations. (**a**) From a double-layer target at near-optimum conditions from the simple theory. (**b**) From a simple proton target. The double-layer target consists of a front carbon ($Z_1 = +4$) layer and rear proton layer. The laser parameters are $I_L = 2.5 \times 10^{21}$ Wcm^{-2}, $\lambda_0 = 1$ μm, and $\omega_0 = 4\lambda_0$. The target parameters are $n_{e1} = 10n_c$, $D_1 = 10\lambda_0$, $d_1 = 1\lambda_0$, $n_{e2} = n_c$, $D_2 = 1\lambda_0$, and $d_2 = 0.05\lambda_0$.

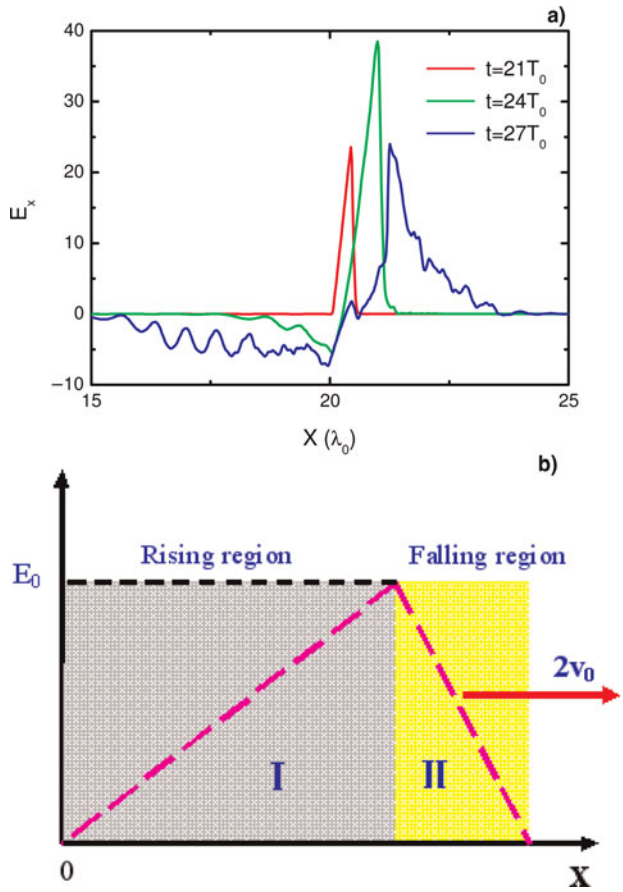

Fig. 2. (Color online) (**a**) Evolution of the space-charge field normalized by $m_e\omega c/e$, where ω is the laser circular frequency. The laser and target parameters are the same as for Figure 1a. (**b**) Sketch of the profile of the electrostatic field (pink dashed line) in the two regions of the simple model.

Case 1 for $v_1 < 2v_0$; before the light ions are sufficiently accelerated, the heavy ions pass them, and neutralize much of the space-charge field, so that the light ions can only gain little energy. Case 2 for $v_1 > 2v_0$; the light ions always remain in front of the heavy ions, so that they are accelerated efficiently in the falling segment of the space-charge field and can achieve high energies with a narrow spectrum because of the narrow acceleration region due to the limited thickness (acceleration distance) of the rear layer. Case 3 for $v_1 \sim 2v_0$; a part of the light ions remains at low speeds in the region I of the space-charge field. Others will be in the region II, where they are compressed and attain high energies with small $\Delta\varepsilon/\varepsilon$, as in Case 2.

In order to see the sensitivity on the charge-to-mass ratio, we have carried out simulations for different charge states of the front-layer heavy ions. The rear-layer light ions are still protons. Figure 3 shows the proton energy spectra, and the electric field and proton density profiles for the charge states $Z_1 = +4$, $+5$, and $+6$. When $Z_1 = +4$ corresponding to Case 2, we see that the accelerated protons have a narrow energy peak around 150 MeV. From the electric field and density profiles, one can see that the protons are in front of the electrostatic field. When $Z_1 = +6$, corresponding to Case 1, the protons are behind the electrostatic field and can only reach a relative low energy of 50 MeV. When $Z_1 = +5$, corresponding to Case 3, there are two peaks in the energy spectrum. From the proton density distribution, we see that a part of the protons are in the falling region of the electrostatic field and these protons can be accelerated to ∼150 MeV. The protons in the ascending region of the space-charge field can only reach 50 MeV. From the simple model, we can calculate the proton speeds. For $Z_1 = +4$, we obtain $v_1 = 0.399c$, which is higher than $2v_0$ ($=0.256c$). For $Z_1 = +6$, we get $v_1 = 0.326c$, which is close to $2v_0$ ($=0.313c$). For $Z_1 = +5$, we have $v_1 = 0.357c$, which is also higher than $2v_0$ ($=0.286c$). Thus, the results obtained from the simple model agree quite well with that from the simulations. In particular, the charge-to-mass ratio of the front layer should not be too large; otherwise the light ions cannot be efficiently accelerated. That is, the ions in the front layer should be heavy enough to make sure a low charge-to-mass ratio, for example, using

https://doi.org/10.1017/S0263034609990218 Published online by Cambridge University Press

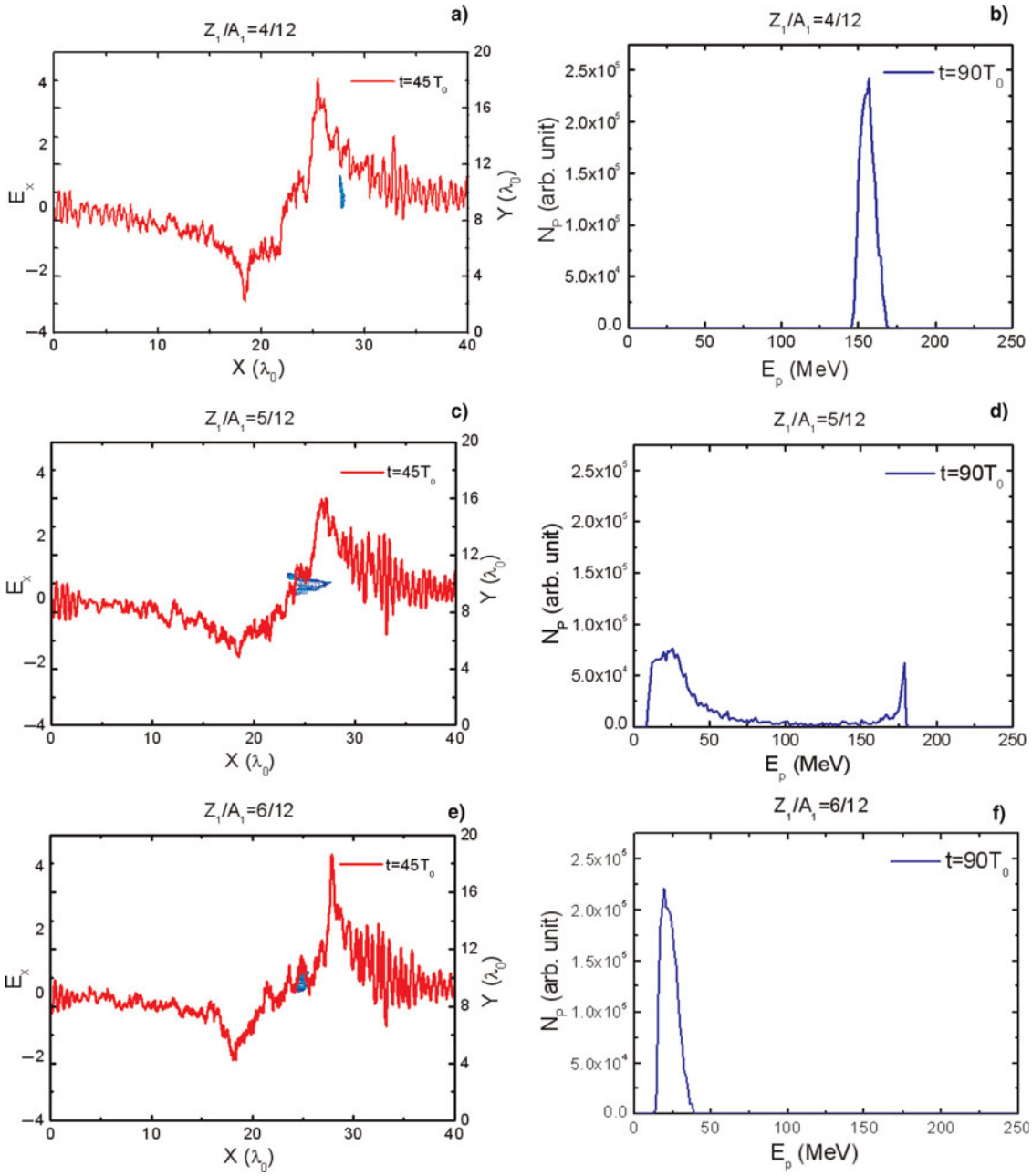

Fig. 3. (Color online) Effect of the charge-to-mass ratio. (**a**) and (**b**) $Z_1/A_1 = 4/12$, (**c**) and (**d**) $Z_1/A_1 = 5/12$, and (**e**) and (**f**) $Z_1/A_1 = 6/12$. The left column shows the space-charge field (red solid lines) at $t = 45T_0$. The profiles (small blue patches) of the nearly monoenegetic proton bunch at the same instant is also shown. The right column shows the proton energy spectra at $t = 90T_0$ (blue solid lines). The laser parameters and the target structure are the same of Figure 1a except that $n_{e2} = 2n_c$.

gold ions in experiments instead of the carbon ions in the PIC simulations.

In each simulation above, the heavy ions in the front-layer are in one charge state. In an experiment, the heavy ions will be field ionized to multiple charge states by the accelerating sheath. In order to see the effect of multiple charge states on the proton energy spectra, we have carried out the simulation with multiple charge states of the front-layer heavy ions. In the simulation, the charge states of the front-layer carbon ions are $Z_1 = +4$ and $+6$. The densities of C^{4+} and C^{6+} ions are $5/4n_c$ and $5/6n_c$, respectively, which results in the electron density in the front layer being $10n_c$. The other parameters are the same of Figure 3. The proton energy spectrum is shown in Figure 4, which still shows monoenergetic characteristics.

We consider now the effect of the thickness of the target layers. Figure 5a shows that proton acceleration is inefficient if the thickness d_1 of the heavy-ion layer is too small, since the space-charge field inside the DL cannot reach a high value. If the heavy-ion layer is too thick, the

https://doi.org/10.1017/S0263034609990218 Published online by Cambridge University Press

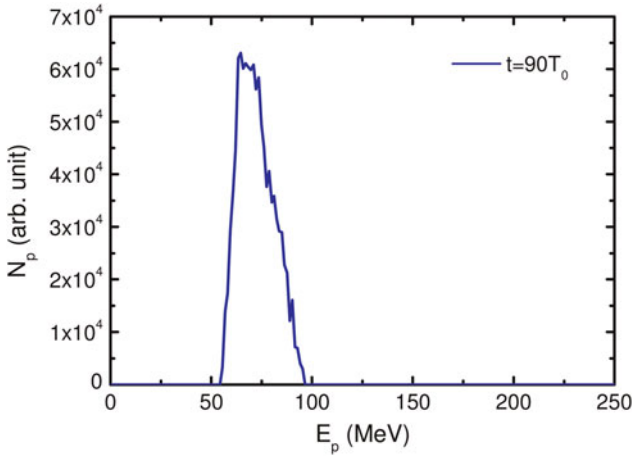

Fig. 4. (Color online) The proton energy spectrum for the front-layer carbon ions with charge states $Z_1 = +4$ and $+6$. The densities of C^{4+} and C^{6+} ions are $5/4n_c$ and $5/6n_c$, respectively. The other parameters are the same of Figure 3.

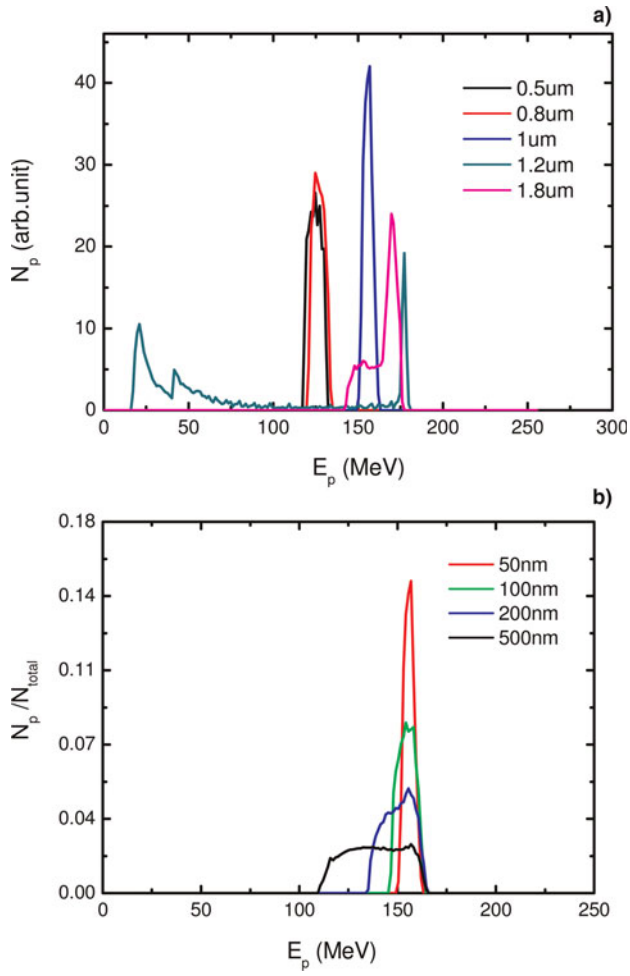

Fig. 5. (Color online) (**a**) The proton energy spectra $t = 90T_0$ for different thicknesses of the front-layer ions. (**b**) The proton energy spectra at the same instant for different thicknesses of the proton layer. Other parameters are the same of Figure 1a.

space-charge field will be partially neutralized by the accelerated heavy ions (corresponding to Case 3), and the protons also cannot gain much energy. Maximum proton energy is obtained when the front-layer thickness is equal to the estimated optimum thickness. Our estimate also shows that the thickness d_2 of the rear, or proton, layer should be close to the skin depth l_s, so that all the protons in the rear layer can be accelerated by the same space-charge field. If the proton layer is too thick, the protons will be accelerated by the space-charge field at different local intensities. In Figure 5b, one sees that with increase of the proton-layer thickness, the proton energy spectrum becomes less monoenergetic. Thus, in order to obtain high quality ion beams, the rear layer should be sufficiently thin.

5. CONCLUSION

In summary, a scheme of monoenergetic light-ion beam generation from the interaction of a circularly polarized laser pulse with a double-layer target is proposed. When the charge-to-mass ratio of the heavy ions is small and the conditions $d_1 \sim d_{opt} = \sqrt{I_L/\pi}c/en_{e1}$ and $d_2 \sim l_s = c/\omega_p$ are satisfied, a high quality monoenergetic proton beam can be generated. The 2D PIC simulation results agree quantitatively with that of a simple model. Our results should be useful in the design of practical applications of the monoenergetic light-ion beams generated by laser-target interaction.

ACKNOWLEDGMENTS

The work was supported by the Natural Science Foundation of China under Grant Nos. 10734130, 10775165, 10875158, and 10835003, the NSAF under Grant Nos. 10876011 and 10676010, the Science and Technology Commission of Shanghai Municipality under Grant No. 08PJ14102, and the JSPS Japan-China Core University Program.

REFERENCES

Borghesi, M., Campbell, D.H., Schiavi, A., Willi, O., Mackinnon, A.J., Hicks, D., Patel, P., Gizzi, L.A., Galimberti, M. & Clarke, R.J. (2002). Laser-produced protons and their application as a particle probe. *Laser Part. Beams* **20**, 269–275.

Breschi, E., Borghesi, M., Campbell, D.H., Galimberti, M., Giulietti, D., Gizzi, L.A., Romagnani, L., Schiavi, A. & Willi, O. (2004). Spectral and angular characterization of laser-produced proton beams from dosimetric measurements. *Laser Part. Beams* **22**, 393–397.

Cobble, J.A., Johnson, R.P., Cowan, T.E., Renard-LeGalloudec, N. & Allen, M. (2002). High resolution laser-driven proton radiography. *J. Appl. Phys*. **92**, 1775–1779.

Davis, J. & Petrov, G.M. (2009). Generation of GeV ion bunches from high-intensity laser-target interactions. *Phys. Plasma* **16**, 023105.

Esirkepov, T.Zh., Bulanov, S.V., Nishihara, K., Tajima, T., Pegoraro, F., Khoroshkov, V.S., Mima, K., Daido, H., Kato, Y., Kitagawa, Y., Nagai, K. & Sakabe, S. (2002). Proposed

https://doi.org/10.1017/S0263034609990218 Published online by Cambridge University Press

double-layer target for the generation of high-quality laser-accelerated ion beams. *Phys. Rev. Lett*. **89**, 175003.

Flippo, K., Hegelich, B.M., Albright, B.J., Yin, L., Gautier, D.C., Letzring, S., Schollmeier, M., Schreiber, J., Schulze, R. & Fernandez, J.C. (2007). Laser-driven ion accelerators: Spectral control monoenergetic ions and new acceleration mechanisms. *Laser Part. Beams* **25**, 3–8.

Hegelich, B.M., Albright, B.J., Cobble, J., Flippo, K., Letzring, S., Paffett, M., Ruhl, H., Schreiber, J., Schulze, R.K. & Fernandez, J.C. (2006). Laser acceleration of quasi-monoenergetic MeV ion beams. *Nat*. **439**, 441–444.

Kado, M., Daido, H., Fukumi, A., Li, Z., Orimo, S., Hayashi, Y., Nishiuchi, M., Sagisaka, A., Ogura, K., Mori, M., Nakamura, S., Noda, A., Iwashita, Y., Shirai, T., Tongu, H., Takeuchi, T., Yamazaki, A., Itoh, H., Souda, H., Nemoto, K., Oishi, Y., Nayuki, T., Kiriyama, H., Kanazawa, S., Aoyama, M., Akahane, Y., Inoue, N., Tsuji, K., Nakai, Y., Yamamoto, Y., Kotaki, H., Kondo, S., Bulanov, S., Esirkepov, T., Utsumi, T., Nagashima, A., Kimura, T. & Yamakawa, K. (2006). Observation of strongly collimated proton beam from tantalum targets irradiated with circular polarized laser pulses. *Laser Part. Beams* **24**, 117–123.

Khoroshkov, V.S. & Minakova, E.I. (1998). Proton beams in radiotherapy. *Eur. J. Phys*. **19**, 523–536.

Klimo, O., Psikal, J., Limpouch, J. & Tikhonchuk, V.T. (2008). Monoenergetic ion beams from ultrathin foils irradiated by ultrahigh-contrast circularly polarized laser pulses. *Phys. Rev. ST AB* **11**, 031301.

Kraft, G. (2001). What we can learn from heavy ion therapy for radioprotection in space. *Phys. Medica*. **17**, 13–20.

Krushelnick, K., Clark, E.L., Allott, R., Beg, F.N., Danson, C.N., Machacek, A., Malka, V., Nakmudin, Z., Neely, D., Norreys, P.A., Salvati, M.R., Santala, M.I.K., Tatarakis, M., Watts, I., Zepf, M. & Dangor, A.E. (2000). Ultrahigh-intensity laser-produced plasmas as a compact heavy ioninjection source. *IEEE Trans. Plasma Sci*. **28**, 1184–1189.

Linz, U. & Alonso, J. (2007). What will it take for laser driven proton accelerations to be applied to tumor therapy. *Phys. Rev. ST AB* **10**, 094801.

Liseikina, T.V. & Macchi, A. (2007). Features of ion acceleration by circularly polarized laser pulses. *Appl. Phys. Lett*. **91**, 171502.

Macchi, A., Cattani, F., Liseykina, T.V. & Cornolti, F. (2005). Laser acceleration of ion bunches at the front surface of overdense plasmas. *Phys. Rev. Lett*. **94**, 165003.

Malka, V., Fritzler, S., Lefebvre, E., d'Humieres, E., Ferrand, R., Grillon, G., Albaret, C., Meyroneinc, S., Chambaret, J.P., Antonetti, A. & Hulin, D. (2004). Practicability of protontherapy using compact laser systems. *Med. Phys*. **31**, 1587–1592.

Nickles, P.V., Ter-Avetisyan, S., Schnürer, M., Sokollik, T., Sandner, W., Schreiber, J., Hilscher, D., Jahnke, U., Andreev, A. & Tikhonchuk, V. (2007). Review of ultrafast ion acceleration experiment in laser plasma at Max Born Institute. *Laser Part. Beams* **25**, 347–363.

Robinson, A.P.L., Zepf, M., Kar, S., Evans, R.G. & Bellei, C. (2008). Radiation pressure acceleration of thin foils with circularly polarized laser pulses. *New J. Phys*. **10**, 013021.

Roth, M., Cowan, T.E., Key, M.H., Hatchett, S.P., Brownl, C., Fountain, W., Johnson, J., Pennington, D.M., Snavely, R.A., Wilks, S.C., Yasuike, K., Ruhl, H., Pegoraro, F., Bulanov, S.V., Campbell, E.M., Perry, M.D. & Powell, H. (2001). Fast ignition by intense laser-accelerated proton beams. *Phys. Rev. Lett*. **86**, 436–439.

Schwoerer, H., Pfotenhauer, S., Jackel, O., Amthor, K.-U., Liesfeld, B., Ziegler, W., Sauerbrey, R., Ledingham, K.W.D. & Esirkepov, T. (2006). Laser-plasma acceleration of quasi-monoenergetic protons from microstructured targets. *Nat*. **439**, 445–448.

Wilks, S.C., Langdon, A.B., Cowan, T.E., Roth, M., Singh, M., Hatchett, S., Key, M.H., Pennington, D., MacKinnon, A. & Snavely, R.A. (2001). Energetic proton generation in ultra-intense laser-solid interactions. *Phys. Plasma* **8**, 542–549.

Xu, H., Chang, W.W., Zhuo, H.B., Cao, L.H. & Yue, Z.W. (2002). Parallel programming of 2(1/2)-dimensional pic under distributed-memory parallel environments. *Chin. J. Comput. Phys*. **19**, 305–310.

Yan, X.Q., Lin, C., Sheng, Z.M., Guo, Z.Y., Liu, B.C., Lu, Y.R., Fang, J.X. & Chen, J.E. (2008). Generating high-current monoenergetic proton beams by a circularly polarized laser pulse in the phase-stable acceleration regime. *Phys. Rev. Lett*. **100**, 135003.

Yin, L., Albright, B.J., Hegelich, B.M. & Fernandez, J.C. (2006). GeV laser ion acceleration from ultrathin targets: The laser break-out afterburner. *Phys. Rev. ST AB* **24**, 291–298.

Yin, L., Albright, B.J., Hegelich, B.M., Bowers, K.J., Flippo, K.A., Kwan, T.J.T. & Fernandez, J.C. (2007). Monoenergetic and GeV ion acceleration from the laser breakout afterburner using ultrathin targets. *Phys. Plasma* **14**, 056706.

Yin, Y., Wei, Y., Yu, M.Y., Lei, A.L., Yang, X.Q., Xu, H. & Senecha, V.K. (2008). Influence of target thickness on the generation of high-density ion bunches by ultrashort circularly polarized laser pulses. *Phys. Plasma* **15**, 093106.

Yogo, A., Sato, K., Nishikino, M., Mori, M., Teshima, T., Numasaki, H., Murakami, M., Demizu, Y., Akagi, S., Nagayama, S., Ogura, K., Sagisaka, A., Orimo, S., Nishiuchi, M., Pirozhkov, A.S., Ikegami, M., Tampo, M., Sakaki, H., Suzuki, M., Daito, I., Oishi, Y., Sugiyama, H., Kiriyama, H., Okada, H., Kanazawa, S., Kondo, S., Shimomura, T., Nakai, Y., Tanoue, M., Sasao, H., Wakai, D., Bolton, P.R. & Daido, H. (2009). Application of laser-accelerated protons to the demonstration of DNA double-strand breaks in human cancer cells. *Appl. Phys. Lett* **94**, 181502.

Zhang, X.M., Shen, B.F., Li, X.M., Jin, Z.Y., Wang, F.C. & Wen, M. (2007). Efficient GeV ion generation by ultraintense circularly polarized laser pulse. *Phys. Plasma* **14**, 123108.

https://doi.org/10.1017/S0263034609990218 Published online by Cambridge University Press